ORIGINAL ARTICLE

Molecular dynamics comparative study of methane–nitrogen and methane–nitrogen–ethane systems

Fouzia Mesli [a]**, Radia Mahboub** [a,*]**, Mourad Mahboub** [b]

[a] *Department of Chemistry, Faculty of Sciences, Abou Bakr Belkaid University, B.P. 119, Tlemcen, 13 000, Algeria*
[b] *Department of Physics, Faculty of Sciences, Abou Bakr Belkaid University, B.P. 119, Tlemcen, 13 000, Algeria*

Abstract   This work concerns the site–site interaction study of 256 particles using the Buckingham potential model. We have calculated the new parameters of the Buckingham potential using an iterative algorithm with a mean square method. This adapted model allows determining the characteristics for each state point. We have applied this model to study the liquefied natural gas LNG properties for methane-nitrogen and methane–nitrogen–ethane mixtures by molecular dynamics. We have calculated the thermodynamic, dynamic and structural properties for both the microcanonical NVT and the isothermal-isobaric NPT ensembles of binary and ternary systems from the SP_1 to SP_9 points. Then, we have compared the results between binary and ternary systems. We have obtained a good prediction on transport properties. From the calculated values of self-diffusion coefficient and viscosity, we have confirmed the liquid state of the liquefied natural gas LNG system.

© 2010 King Saud University. Production and hosting by Elsevier B.V. All rights reserved.

1. Introduction

Molecular dynamics (MD) is a talented technique which consists in modelling a simulation of macroscopic systems involv-

* Corresponding author.
  E-mail address: radiamahboub@yahoo.com (R. Mahboub).

ing a few molecules. Nowadays, molecular dynamics tends to become an alternative to experiments in order to provide transport properties (Morriss et al., 1991; Padilla and Toxvaerd, 1992). These processes happen in many cases extremely variables in the time and the space. Because these phenomenons are irreversible, they occur in material systems at the equilibrium state. Favour to thermal agitation, they can transport a molecular size like as matter, energy and quantity of movement.

The liquefied natural gas (LNG) is a subject of numerous studies. The LNG properties have frequently been investigated because of their industrial importance. LNG consists predominantly of methane (95%). It will contain higher fraction of ethane (3%) and some propane. We quote the works of Murad et al. (1979) which concern the study of the liquid methane by simulation of molecular dynamics. We also find the works of

simulation by MD of Habenschuss et al. (1981) whom studied the site–site interaction of the liquid methane.

Recent studies of thermodynamic, structural and of transport properties by MD simulation have just been finalized the modelling and statistical simulation methods of quantum chemistry. These computations involve the study of the rigid methane molecule in the spherical interaction (Tchouar et al., 1998), and in the site–site interaction (Belkacem et al., 2005). The Gibbs ensemble is a simulation technique developed specifically for the study of phase equilibrium prediction of thermodynamic and structural properties of mixtures by different numerical methods as Monte-Carlo (MC) (McDonald and Singer, 1972; Sesé, 1992; Kincaid and Scheraga, 1982) and molecular dynamics (MD) (Murad et al., 1979; Nicolas et al., 1979). Different approaches derived from Monte-Carlo simulation involve the Quadratic Feynmann–Hibbs (QFH) (Sesé, 1993), the Gaussian Feynmann–Hibbs (GFH) effective potentials, the Path-Integral Monte-Carlo (PIMC) (Berne and Thirumalai, 1986), the Path-Integral Brownian Dynamics (PIBD) (Singer and Smith, 1988), and the other Path-Integral methods (PIBC) (MS–PI) (Powles and Abascal, 1983). In these calculations, different properties are obtained for the methane interactions and supposed that the system is spherical (Tchouar et al., 2003).

In our earliest work, we have studied the different properties of CH_4–N_2 system by MD at the SP_1, SP_4, and SP_8 points (Mesli and Mahboub, 2010). Here, we apply the same method for complex systems. So, we are interested in binary (CH_4–N_2) and ternary (CH_4–N_2–C_2H_6) mixtures from the SP_1 to SP_9 points. We detail in this article the various techniques of simulation which make it possible to study the phenomenon of transport. We will present here recent results on the thermo-diffusion of binary and ternary mixtures of hydrocarbons. To perform this search and to approach the reality, we have taking into account of all the site–site interactions between molecules.

This study is realized on the mixtures of methane-nitrogen and methane-nitrogen-ethane systems. In this case, the study is very complex because it concerns to build a model of 2 sites for the nitrogen, 5 sites for the methane and 8 sites for the ethane. So, we have numerically simulated the site–site interactions of binary and ternary mixtures to visualise the evolution of our systems in the time. Moreover, our study is carried simulations for both canonical NVT and isothermal-isobaric NPT systems in order to evaluate thermodynamic, structural and transport properties of LNG constituents and to optimise the liquefaction process.

In this work, we have applied the new Buckingham potential model to binary (CH_4–N_2) and ternary (CH_4–N_2–C_2H_6) systems. We have preferred the Buckingham model because all site–site interactions of molecules (C···C, C···H, H···H, N···H, N···N and C···N) in the mixture are kept of bond environments comparatively of classical approach which considered only the spherical interactions. The new results are compared with those of literature, especially with Williams work relative to lattice energy of hydrocarbons.

In Section 2 of this paper, we give the numerical model for the Buckingham potential. We have determined Buckingham potential parameters by adjusting the two curves (LJ and Buckingham) until the total minimization of potential energies have been occurred. Radial distribution functions are described in Section 3 to determine the structural properties of LNG constituents. In the same section, the properties of transport are calculated from temporal correlation functions. In the next section, we have studied the evolution of the various thermodynamic properties of binary (CH_4–$N_2$$CH_4$–$N_2$) and ternary ($CH_4$–$N_2$–$C_2H_6$) systems, for two units NVT and NPT from the SP_1 to SP_9 points. We give our comparative study in Section 4 and we present the conclusion in Section 5.

2. Numerical model

In literature, much potential are proposed (Sesé, 1991; Catlow and Harker, 1975; Nagy et al., 1995). The first potential having a theoretical significance is the inverse potential (Maghri and Jalili, 2004). Hoover has used the nine, six, and four inverse potentials to study the transition phase fluid-solid (Evens and Morriss, 1984). After, the searchers have employed the square well potential. Consider it insufficiency; scientists have preferred Lennard-Jones potential for the spherical interactions (Lennard–Jones, 1924) and Buckingham potential for the site–site interactions (Mirsky et al., 1978; Buckingham, 1938). There are two other potentials: Exponential-6 (Evens and Hoover, 1986), and Kihara (1963) which are recommended in the spherical interaction studies (Shadman et al., 2009).

From these tools, we can simulate the macroscopic phenomenon in order to understand the physical properties. The simulation must establish a band between the macroscopic properties and intermolecular forces. So, the interaction potential model used must approach the real physical system. In the present work, we have studied methane-nitrogen and methane-nitrogen-ethane systems by MD using the new model based on the Buckingham potential. Then, we have compared the results between binary and ternary systems.

In this work, we have studied the methane-nitrogen and the methane-nitrogen-ethane mixtures which consist of 256 molecules in freely rotating state. In these calculations, all site–site interactions (C···C, C···H, H···H, N···H, N···N and C···N) between any two separated molecules are considered through the site–site model of Buckingham (Buck) model.

We have preferred the potential of Buckingham (Buck) because it: (i) takes of all bond interaction environments, (ii) has been frequently used to describe the non-bonded energy interaction between united atoms, and (iii) used for the study of the complex systems (Eq. (1)):

$$U(r) = B_{ij}e^{-C_{ij}r} - \frac{A_{ij}}{r^6} \qquad (1)$$

where A is the size parameter, B is the energy parameter, C is the gradient parameter in the exponential repulsion term and r is the distance between the centers of molecules mass.

We have calculated the new A, B, and C parameters by our method which we describe hence. Williams has only determined the parameters A, B, and C for C···C, H···H, and C···H interactions (Narten and Levy, 1972) from crystal lattice energies of hydrocarbons (Williams, 1967). The distance between the C and H sites is 1.026 Å in Williams's model. This value is less than the distance between the C and H nucleus (the usual bond length is 1.094 Å).

First, we have taken the Lennard-Jones potential parameters: σ (interaction diameter) and ε (depth of well) from literature (Lennard-Jones, 1924), for estimate the C···C, H···H, and C···H interactions (Eq. (2)):

$$U_{LJ}(r) = 4\varepsilon \left[\left(\frac{\sigma}{r} \right)^{12} - \left(\frac{\sigma}{r} \right)^6 \right] \qquad (2)$$

where the r is the distance between the centers of molecules mass.

Secondly, we have used from literature the parameters σ and ε, for N···N interaction (Allen, 1987). To determine the new σ and ε parameters for C···N and N···H interactions, we have used the standard Lorentz–Berthelot combining rules to calculate the interactions between unlike molecules:

$$\varepsilon_{ij} = \sqrt{\varepsilon_i \varepsilon_j}, \sigma_{ij} = \frac{(\sigma_i + \sigma_j)}{2} \qquad (3)$$

Finally, to estimate the new Buckingham A, B, and C values, we have adjusted by an iterative algorithm with a mean square method, the two curves (LJ and Buckingham) until the total minimization of potential energies has been occurred. In Table 1, we give all the site–site potential parameters in real units.

The thermodynamic functions (temperature and density) are calculated as follow: $T^* = T \cdot K_B/\varepsilon$, $\rho^* = \sigma^3$, $\rho = \sum \rho_i X_i$, and $\sum X_i = 1$, for the nine state points of the methane-nitrogen and methane-nitrogen-ethane mixtures (Table 2).

- K_B: Boltzmann constant, ρ_i: density for constituent i and X_i: molar fraction for constituent i.
- CH$_4$–N$_2$: $X_{CH_4} = 0.600$ and $X_{N_2} = 0.400$.
- CH$_4$–N$_2$CH$_4$–N$_2$–C$_2$H$_6$: $X_{CH_4} = 0.500$, $X_{N_2} = 0.200$ and $X_{C_2H_6} = 0.300$.

- MCRB: $X_{CH_4} = 0.42$ and $X_{N_2} = 0.03$.
- MCRT: $X_{CH_4} = 0.55$, $X_{N_2} = 0.03$ and $X_{C_2H_6} = 0.4$

The cutoff distances for the Lennard–Jones intermolecular potentials were always $2.5\sigma_{ij}$. The overall runtime is 100 ps with an equilibration period of 50 ps and data production period reaching up to 50 ps to ensure a good accuracy in calculated ensemble averages of most properties. Calculations are performed for both the microcanonical NVT ensemble and the isothermal-isobaric NPT ensemble. In the previous, the Nosé thermostat process is applied, whereas the isothermal-isobaric NPT incorporate the Parinnello–Raman integration scheme. The equations of motion (both for the translation and rotation) are solved using the fifth order Gear predictor and periodic boundary conditions around the central cubic box and the minimum image truncation were included in the calculations, long-range corrections are also applied. The integration scheme uses a constant time step algorithm $\Delta t = 5$ fs.

When the equilibrium is reached, several properties are calculated: pressure P, energy of configuration U, enthalpy H, and pair correlation function (Allen, 1987). The self-diffusion coefficient D was obtained from the slop of the mean square displacement as function of time, at long time (Hansen and McDonald, 1986). The viscosity coefficient η was evaluated from Green–Kubo integral of the computed stress correlation function (Hansen and McDonald, 1986).

Table 1 Potential parameters of site–site interactions for C···C, C···H, H···H, N···H, N···N and C···N.

Potential parameters	LJ			Buckingham		
	σ_{ij} (Å)	ε_{ij}/k_B (K)	ε_{ij} (Kcal/mol)	A_{ij} (Kcal/mol Å^{-6})	B_{ij} (Kcal/mol)	C_{ij} (Å^{-1})
C. . ..C	3.35	50.00	0.09930	524.690	79498.56	3.663
C. . ..C[a]	–	–	–	505.000	61900.00	3.600
C. . ..H	3.08	20.73	0.04120	123.230	94603.00	4.329
C. . ..H[a]	–	–	–	128.000	11000.00	3.670
H. . ..H	2.81	08.60	0.01700	31.799	96526.01	2.990
H. . ..H[a]	–	–	–	32.300	26290.00	3.740
N. . ..N	3.31	37.30	0.07413	550.000	236699.52	3.310
C. . ..N	3.33	43.18	0.08581	549.760	181197.32	3.330
H. . ..N	3.06	17.91	0.35590	659.330	705500.21	3.040

[a] Work reported by Williams (Narten and Levy, 1972).

Table 2 Type of fluids and thermodynamic state points. Temperatures and Densities in real and reduced units.

State point	T (K)	T^*	ρ (g/cm^3)						ρ^*		
			CH$_4$	N$_2$	C$_2$H$_6$	CH$_4$ N$_2$ LNG	CH$_4$–N$_2$ MCR	CH$_4$–N$_2$–C$_2$H$_6$ MCR	CH$_4$–N$_2$ LNG	CH$_4$–N$_2$ MCR	CH$_4$–N$_2$–C$_2$H$_6$ MCR
SP$_1$	91.0	0.6103	0.4495	0.7401	0.6537	0.2697	0.2109	0.5439	0.5310	0.4152	1.0708
SP$_2$	99.8	0.6692	0.4407	0.6892	0.6160	0.2644	0.1889	0.5216	0.5206	0.3719	1.0269
SP$_3$	105.4	0.7069	0.4331	0.6572	0.6363	0.2598	0.2016	0.5251	0.5115	0.3969	1.0338
SP$_4$	108.0	0.7243	0.4263	0.6346	0.6334	0.5557	0.1980	0.5194	0.5034	0.3898	1.0226
SP$_5$	110.9	0.7437	0.4253	0.6131	0.6291	0.2551	0.1970	0.5164	0.5022	0.3878	1.0167
SP$_6$	116.5	0.7813	0.4173	0.5677	0.6224	0.2503	0.1922	0.5079	0.4928	0.3784	0.9999
SP$_7$	122.1	0.8189	0.4091	0.5076	0.6182	0.2454	0.1870	0.4998	0.4831	0.3682	0.9840
SP$_8$	125.0	0.8284	0.4005	0.4851	0.6124	0.2403	0.1827	0.4919	0.4731	0.3597	0.9684
SP$_9$	127.6	0.8558	0.4006	0.4586	0.6101	0.24036	0.1820	0.4902	0.4732	0.3853	0.9651

3. Results and discussions

We have realised our simulation from the SP_1 to SP_9 points taken from the phase diagram (Tchouar et al., 1998) using the Buckingham potential model. The mixtures of methane–nitrogen and methane–nitrogen–ethane are taken to be rigid. All the site points are covered by molecules to interact through the Buckingham site–site potential. Then, we have compared the obtained properties for the binary and ternary systems.

Using an approach by numerical simulation of molecular dynamics, we have studied the evolution of the various structural, transport and thermodynamic properties of the CH_4–N_2 and CH_4–N_2–C_2H_6 mixtures in both NVT and NPT systems using the cited potential model.

3.1. Structural properties

The structural properties $g(r)$ are calculated to describe the average structure of the fluid. The site–site correlation function $g(r)$ is proportional to the probability density of finding the β site of some molecule at a distance $r_{\alpha\beta}$ from the α site of some different molecule. It is given in terms of the angular pair correlation function (Allen, 1987; Streett and Gubbins, 1977; Lowden and Chasndler, 1974).

The equation of $g(r)$ can be easily obtained from equation cited in reference (Lowden and Chasndler, 1974)

$$g\left(r_{\alpha\beta}\right) = < g\left(r_{\alpha\beta} + r_{c\alpha1} - r_{c\beta2}; w1w2\right)>_{w1w2} \tag{4}$$

where r is the vector from site α in molecule 1 to site β in molecule 2, $r_{\alpha\beta}$ is the vector from the centre of molecule 1 to site α, and $<\cdots>_{w1w2}$ is an outweighed average over the molecular orientations. The resulting site–site correlation functions $g(r)$ are shown in Fig. 1.

All these figures give us significant structural information for both the NPT and NVT systems. The radial distribution function forms inform us that all the interactions occur in liquid state. For the two figures (Fig. 1a and b), the NPT system characterizes much better as for the binary as the ternary system than the NVT one. So, we have obtained similar results with those of Murad et al. (1979). In addition, the curves of the ternary system present many sketches which are absent in the binary system. Ternary mixture has multi-components with numerous interactions.

In Fig. 2, we have given the most important orientations responsible for the peaks. So, we have only drawn the configurations which reproduced the picks of radial distribution functions in Fig. 1 obtained by MD. These configurations were drawn using the ACD/ChemSketch.

For the H$\cdots$H interaction, we have considered two molecules of methane or ethane in position such two atoms of hydrogen and β are in contact. The distance r_1 between the α hydrogen in molecule1 and the atom γ hydrogen in molecule 2 (with α and are in contact) reaches its maximum. This situation corresponds to the peak in $g(r)_{HH}$. The highest separation is happening when the three atoms: α, β and γ are collinear (configurations 1-A and 1-B in Fig. 2). This separation is self-sufficient from the orientation of molecule1 around its α hydrogen atom.

The configurations responsible of the peaks in Fig. 1 are shown in the representations 2-A, 2-B and 3-A, 3-B for the H$\cdots$C and respectively C$\cdots$C interactions which are represented by the distances r_2 and r_3 (Fig. 2).

From the configurations 1-C, 2-C and 3-C, we observe that the distances r_4 and r_5 are independents of molecule orientation around its site axis. These are relatives to the C$\cdots$N and H$\cdots$N interactions.

From these results, we confirm that the discontinuities and the peaks in the site–site correlation functions are the consequence of the intermolecular potential Buckingham model. So, these characteristics are obvious in the ternary system because the Buckingham potential takes of all bond interaction environments.

The average number neighbours $n(R)$ for a molecule is obtained from the following equation:

$$n(R) = 4\pi\rho \int_0^R r^2 g(r)dr \tag{5}$$

where the integration limit R is taken as the position of successive minima in $g(r)$.

When the value of r becomes close to the diameter of collision, $g(r)$ increases quickly until the maximum $r = r_{max}$. When the separation r continues to increase $g(r)$ decreases which imply that at long distance the influence of the central molecule disappeared. The advantages of these curves allow us to calculate the position of the various maxima and minima and the number of close neighbour. This last one is obtained by integration of the radial distribution function.

The obtained value of this number is compared to the experience measured by X-rayon diffraction which giving a first peak equals to 12 and the second peak equals to 55 (Habenschuss et al., 1981). Sesé (1991) has obtained him results from quantum simulations. The first maximum is $R_{max1} = 4.05$ Å for the three state points. The second maximum is $R_{max2} = 5.75$ Å for SP_1 and $R_{max2} = 5.85$ Å for SP_4 and SP_8. The first minimum for the three state points is $R_{min1} = 7.75$ Å. or the binary and ternary systems, the number of nearest neighbours is 26.25 molecules and in the second layer the number of neighbours is 56.55 molecules.

In the present calculations, similar radial distribution functions for the points SP_1, SP_4, SP_8 are compared with an identical location of the peak positions. The first maximum is $R_{max1} = 4.236$ Å for the binary system, and $R_{max1} = 4.0.25$ Å for the ternary system. The second maximum is $R_{max2} = 7.354$ Å for the binary and $R_{max2} = 7.556$ Å for the ternary systems. However, the first minimum is $R_{min1} = 5.456$–5.542 Å for the three state points of binary system. The first minimum is $R_{min1} = 5.652$–5.765 Å for the three state points of ternary system. Our simulation results of both the binary and ternary systems agree very well with experiment and theoretical works. All these results are regrouped in Table 3.

3.2. Transport properties

The properties of transport are studied by MD and determined by the formalism of Green–Kubo (Sesé, 1994). The last one describes the phenomenological coefficients mainly the coefficient of diffusion and the viscosity. The two parameters are calculated from temporal correlation functions.

The viscosity η is calculated from the integration of the stress autocorrelation function. For the precise values, the viscosity can be calculated by averaging these results from the stress tensor. We have calculated the viscosity as follow:
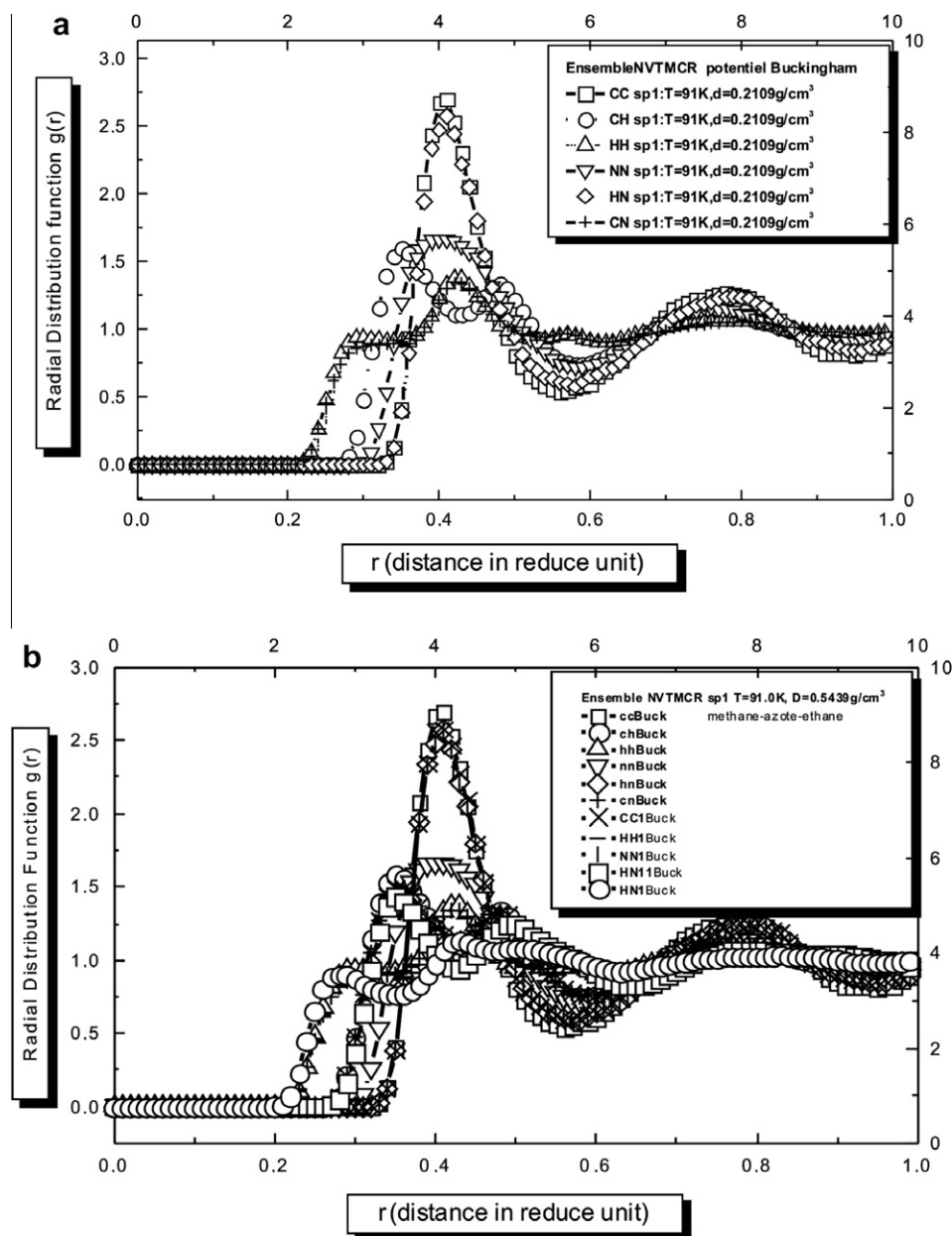
Figure 1 Radial distribution functions of site–site interactionsite–site interaction in NVT system at SP_1 point. (a) CH_4–N_2. (b) CH_4–N_2–C_2H_6.

$$\eta = \frac{V}{10 K_B T} \int_0^{\infty} < P(t)P(0) > dt \tag{6}$$

where V is the system volume, T the temperature, K_B the Boltzmann constant, and P the symmetric traceless pressure tensor (Dysthe et al., 1998, 1999; Cooper, 1965). The last factor allows obtaining the dynamic viscosity of environment.

The stress autocorrelation functions of binary and ternary mixtures are reported in Fig. 3. In the binary system and at the state point SP_1 (Fig. 3a), the curves provide a stable situation in the time because of the increased iteration number. The situation is completely reversed in the ternary (Fig. 3b). The stress autocorrelation function becomes negative for the molecular displacement around the YZ and ZZ stress tensor elements. We think that this situation presents an instable state

at small period. We can confirm that the binary system gives good results with a high precision than the ternary. Therefore, the stress autocorrelation function sums all particles in MD box.

In Fig. 4, we give the viscosity of CH_4–N_2 and CH_4–N_2 CH_4–N_2–C_2H_6 systems at the state point SP_1. The viscosity of binary system is biggest than in the ternary system. The last one is more dense, and it contains numerous compounds ($\rho_{CH_4-N_2} = 0.2109$ g/cm^3 and $\rho_{CH_4-N_2-C_2H_6} = 0.5439$ g/cm^3).

The coefficient of distribution gives the information of diffusion of molecule for the liquid state. There values are positioned between 10^{-9} and 10^{-10} m^2/s. At high temperatures, the molecules have an important kinetic energy which increases the distribution of the particles of methane in the mixture liquid.
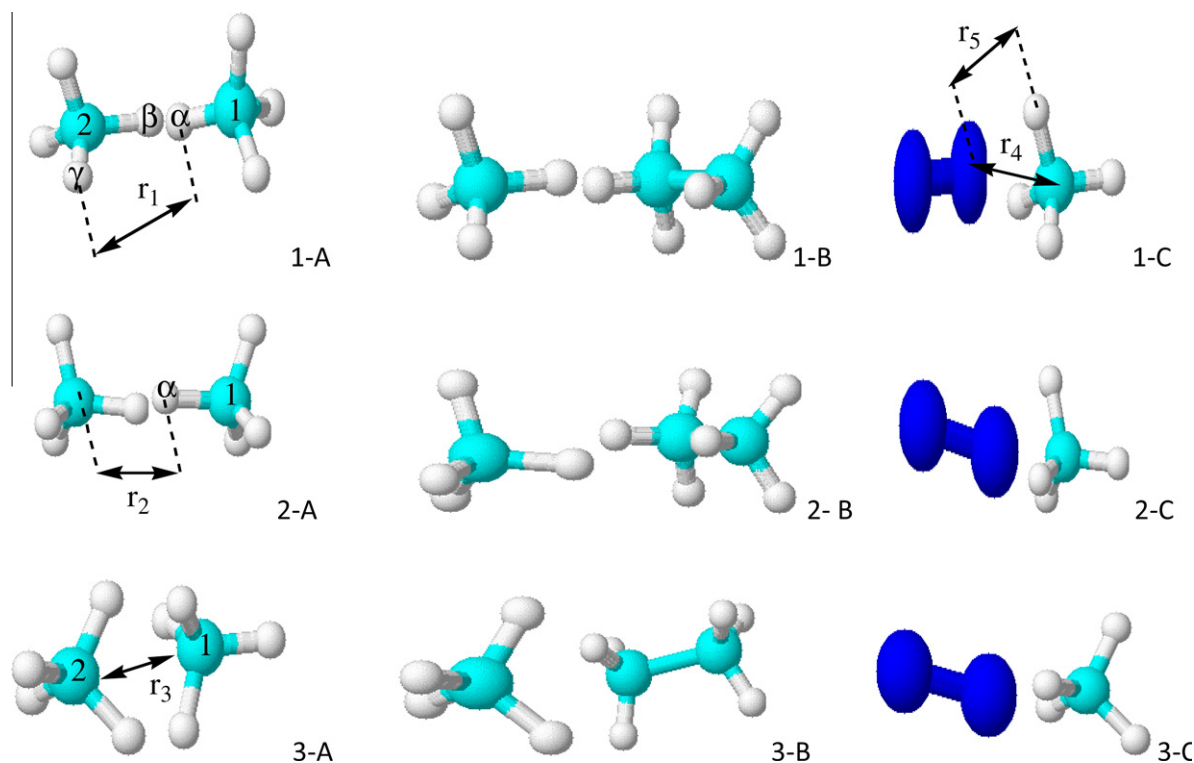
Figure 2   Main pair interactions of two molecules: (A) CH_4–CH_4, (B) C_2H_6–CH_4, and (C) N_2–CH_4.

Table 3   Values of maximum and minimum for $g(r)$ C···C.

State point	R_{max1} (Å)	R_{max2} (Å)	R_{min1} (Å)
SP1, SP4, SP8[a]	4.100	7.700	5.700−5.750
SP1, SP4, SP8[b]	4.050	7.750	5.750−5.850
SP1, SP4, SP8[c]	4.050	7.750	5.750−5.850
SP1, SP4 SP8[d]	1.050	1.750	−
SP1, SP4, SP8[e] MCRB	4.236	7.354	5.456−5.542
SP1, SP4, SP8[e] MCRT	4.025	7.556	5.652−5.765

MCRB: multi-component refrigerants for a binary mixture.
MCRT: multi-component refrigerants for a ternary mixture.
[a] Site–site interaction (Belkacem et al., 2005).
[b] Spherical approximation (Tchouar et al., 1998).
[c] Sesé work (Sesé, 1992, 1994).
[d] Experimental work (Sesé, 1992, 1993, 1994).
[e] Present work.

The self-diffusion coefficient of liquid mixture D is obtained from the mean square displacement (MSD) at long times by the relation of Einstein (Allen, 1987) and the Green–Kubo method (Dysthe et al., 1998, 1999; Cooper, 1965)

$$D = \frac{1}{6N} \lim_{t \to \infty} \frac{d}{dt} \langle \sum_i^N [r_i(t) - r_i(0)]^2 \rangle \qquad (7)$$

where the $r_i(t)$ are the positions of particles at time t and N is the number of molecules in the system.

The mean square displacements of methane-nitrogen and methane-nitrogen-ethane mixtures at point SP_1 are reported in Fig. 5. The variation of the autocorrelation function is observed with linearly rising MSD until the equilibrium is reached. As time increases, an important gap appears between the two curves for the isothermal-canonical system (NVT).

Through the binary CH_4–N_2CH_4–N_2 system, we observe a precise molecular displacement. We note also that this displacement is sluggish than one obtained with the ternary CH_4–N_2CH_4–N_2–C_2H_6 system. So, the simulation time is large and important for the calculations in CH_4N_2 system. In this case, the ternary model is very complex because it concerns of 2 sites for the nitrogen, 5 sites for the methane and 8 sites for the ethane. So, this system takes into account of all theses site interactions of molecule environments.

The formal Green–Kubo theory for D_{ij} in multi-component mixtures has been developed by Zhou and Miller (1996). We have used Eq. (8) in our calculations.

$$D_{ij} = \frac{V}{3NW_iW_jm_im_j} \int_0^\infty < J_i(t)J_j(0) > dt \qquad (8)$$

where V: system volume, N: total number of molecules, W_i: mass fraction, m_i: molecular mass, and J_i: mass flux of component i.

We have done the MD calculations for determining the evolution of self-diffusion coefficients of mixtures CH_4–N_2CH_4–N_2 and CH_4–N_2CH_4–N_2–C_2H_6 for the two NVT and NPT systems at the point SP_1 (sensitive state).

In the NPT ensemble, the values of diffusion coefficient are better than in NVT ensemble. In the first system, the volume fluctuates, the molecules diffuse easily with an important rate through the liquefied natural gas and the pressure is fixed along the simulation time.

Different results of nitrogen-n-pentane are established by two different models AUA (anisotropy united atom) and OPLS (optimised potentials for liquid simulation) (Rowlinson, 1969). There is a qualitative difference between the two models.
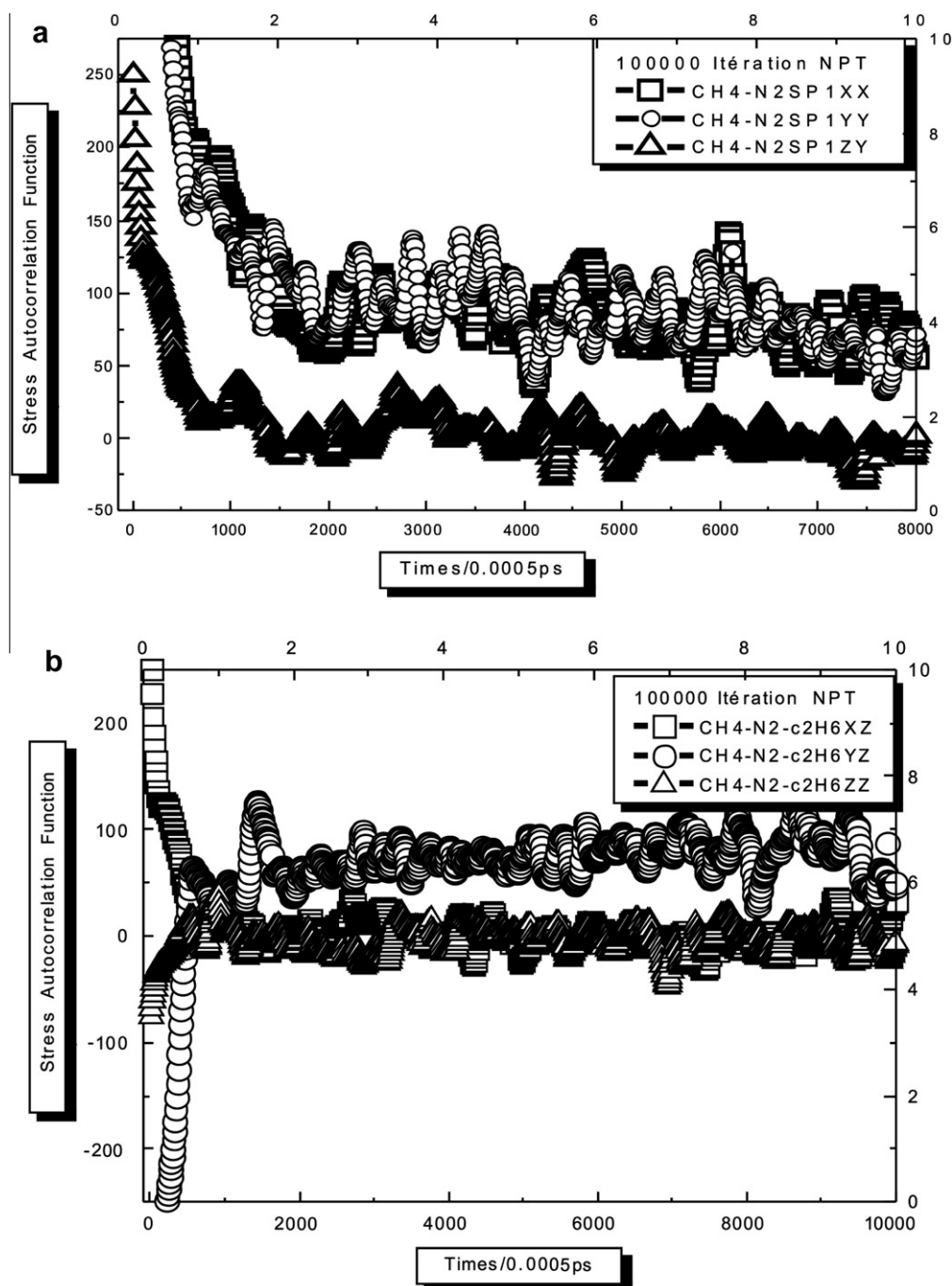
Figure 3 Stress autocorrelation function at the state point SP$_1$. (a) Binary system. (b) Ternary system.

The OPLS model has a LJ spherical interaction centred on the carbon with a large diameter than the AUA model which has the site–site interaction displaced to the geometric centre of the valence electrons for the CH group (Erpenbeck, 1988).

For the mixture n-pentane–nitrogen, and under the following experimental conditions ($T = 325.25$ K, $d = 0.711$ g/cm^3, $P = 120.5$ MPa), the values of coefficient of diffusion found by OPLS and AUA are respectively $(3.44 \pm 0.05)10^{-9}$m^2/s and $(3.87 \pm 0.04)10^{-9}$m^2/s, and those of viscosity are respectively (0.39 ± 0.02) MPa s and (0.31 ± 0.02) MPa s. We carried out our simulation at the same point states (temperature, pressure and density), for the two systems methane-nitro-

gen and methane-nitrogen-ethane in order to compare our result with the contribution quoted before.

Our calculations give us, the values of the coefficient of diffusion for the binary and ternary mixtures are respectively equal to (3.620 ± 0.030) 10^{-9}m^2/s and $(3.705 \pm 0.030)10^{-9}$m^2/s, and those of viscosity are correspondingly (0.257 ± 0.045) and (0.107 ± 0.033) MPa s. We note that ours results for the diffusion are intermediaries between the results of OPLS and AUA.

For the CH$_4$–N$_2$ mixture, the diffusion value decreases because it is more viscous than the CH$_4$–N$_2$–C$_2$H$_6$ mixture (Fig. 6). From these results, we confirmed that more the fluid
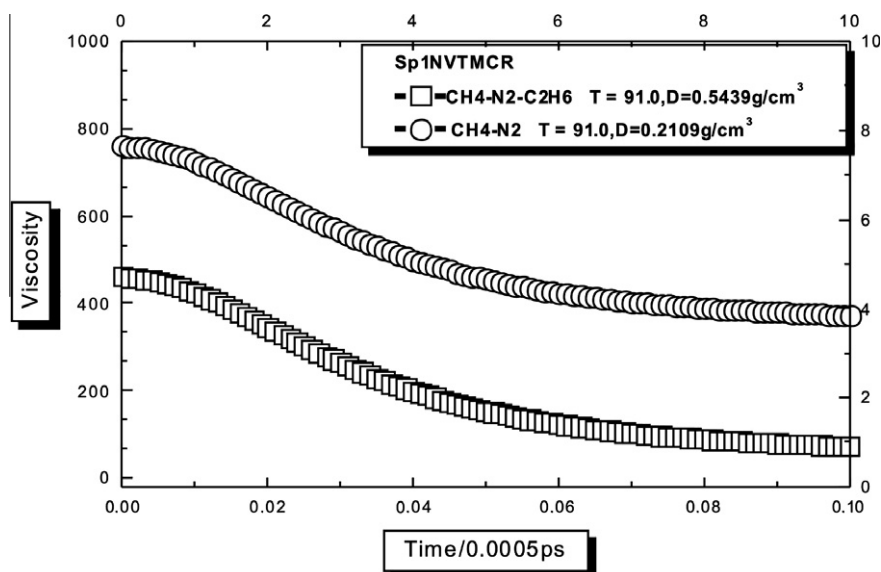
Figure 4   Viscosity of CH_4–N_2 and CH_4–N_2–C_2H_6 in NVT system at the state point SP_1.
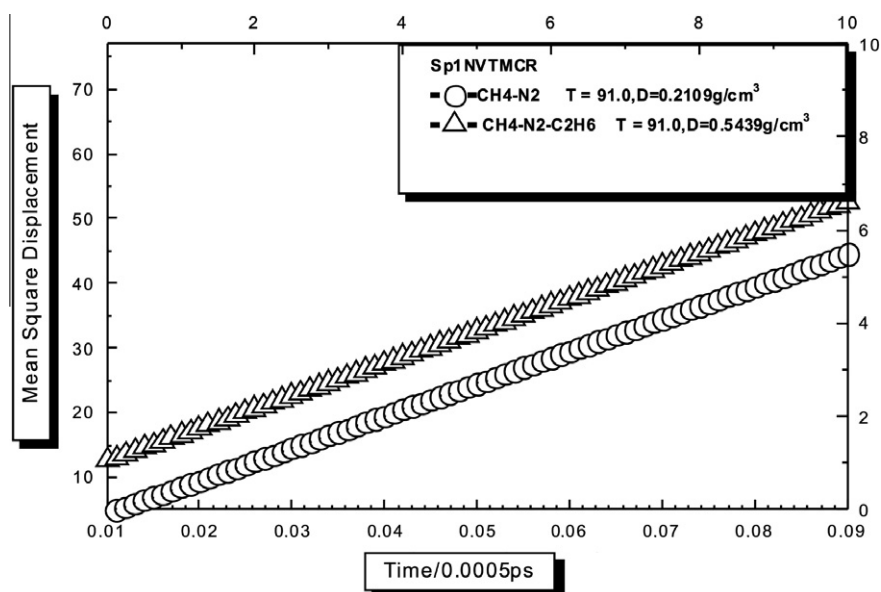
Figure 5   Mean square displacement of CH_4–N_2 and CH_4–N_2–C_2H_6 in MCR at the point SP_1.

is dense more it diffusion coefficient in the liquid will be strong. So, the diffusion of methane in the ternary mixture is much better than in the binary mixture. However, the situation for viscosity is reversed.

3.3. Thermodynamic properties

Using the numerical simulation of molecular dynamics, we have studied the evolution of the various thermodynamic properties of binary (CH_4–N_2CH_4–N_2) and ternary (CH_4–N_2–C_2H_6) mixtures in the NVT and NPT ensembles.

Understanding that the triple point of methane is 90.1 K, of nitrogen is 63.16 K, and this of ethane is 89.89 K, we have realised our calculations near the triple point which is 91 K (Rowlinson, 1969). So, we have chosen nine points from SP_1

until SP_9 which are taken from the phase diagram. In order to minimise the machine execution time of, we have preferred to compute this simulation in reduced units.

The thermodynamic properties (U^*, H^*, P^*) and dynamic properties (D^*, η^*) are calculated in reduced units from the related references (Allen, 1987; Hansen and McDonald, 1986). All our results are given in Table 4.

From Table 4, many characteristics are determined. First, we can confirm the liquid state of the mixture from the values which are around 10^{-9}. At high temperature (from SP_1 to SP_9) the coefficient of diffusion increases. The molecules possess an important energy of configuration to make easy their diffusion through the liquid.

We have found that diffusion coefficient is insensitive to the attractive site–site interaction (Dysthe et al., 1998). Therefore,
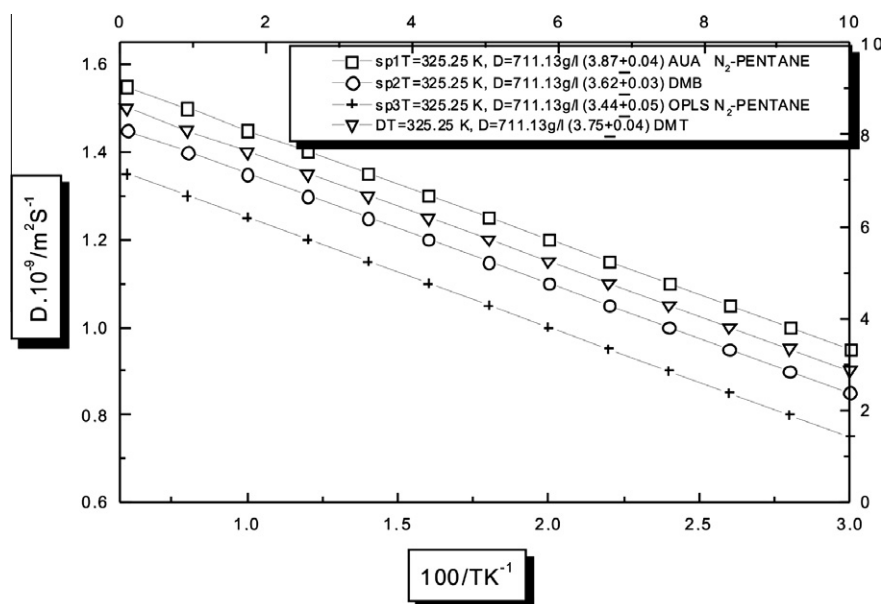
Figure 6 Diffusion coefficient as a function of temperature for the methane–nitrogen, methane–nitrogen–ethane and n-pentane–nitrogen mixtures.

we attribute the increasing deviation in the mixture to steric shape size effects of the molecular cross interactions.

Except the deviations of intra-diffusion coefficients are very sensitive to the cross interactions. The intra-diffusion of the light component is high at low concentrations of nitrogen and methane. However, the situation is reversed at low concentrations of nitrogen.

The viscosity is not very sensitive to cross interactions of species because it is an approximate prediction as for mixture as for pure components (Erpenbeck, 1988). For the two systems, the viscosity decreases by increasing the temperature. So, the self-diffusion coefficient increases then the system will be less viscous. Therefore, the ternary system has the biggest values than the binary system because of the number of components.

Different observations can be made for all state points. Therefore, for the CH_4–N_2–C_2H_6 system, we have found that the reduced energy of configuration U^*, and the reduced enthalpy H^* are not different for both NVT and NPT calculations, but for N_2–CH_4 in MCR they are different. The situation is the same for N_2–CH_4 in LNG except for points SP_1, SP_4 and SP_8.

We conclude that at any moment the energy of configuration is controlled and is invariable in the time. The temperature and the pressure remain fixed in the MCR (isotherm-isobar system). A rising in temperature allows the energy of configuration to the large values. It shows, That MCR gives very precise results for NPT comparing to NVT system.

The fluctuations obtained on the coefficients of diffusion for every state point are situated around a constant value. The fluctuations are high for the pressures and less for the energies of configuration and enthalpies. So, we can confirm that the pressure given in NVT is fixed. The fluctuations on viscosities increase with the diminution of the temperature.

In the ternary mixture steric shape size effects of the molecular cross interactions are important than in the binary mixture. We confirm that the adapted Buckingham potential takes into account of all bond interaction environments.

4. Comparative study

In general, our calculated values are in perfect concordance with those obtained by Sesé (1992). For the points SP_4 and SP_8, our results have a big similarity with the path-integral method (PIMC) for the ternary system. Therefore in the binary system, the situation is comparable to the quantum approach of Wigner-Kirkwood (WK) (Sesé, 1991, 1992, 1993; Kincaid and Scheraga, 1982; Nicolas et al., 1979; Berne and Thirumalai, 1986; Singer and Smith, 1988; Powles and Abascal, 1983; Tchouar et al., 2003; Mesli and Mahboub, 2010; Catlow and Harker, 1975; Nagy et al., 1995; Maghri and Jalili, 2004; Evens and Morriss, 1984; Lennard-Jones, 1924; Mirsky et al., 1978; Buckingham, 1938; Evens and Hoover, 1986; Kihara, 1963; Shadman et al., 2009; Narten and Levy, 1972; Williams, 1967; Allen, 1987; Hansen and McDonald, 1986; Streett and Gubbins, 1977; Lowden and Chasndler, 1974; Sesé, 1994). However, we have examined the exception for the point SP_1 for the two systems. The point SP_1 is very sensitive state because it is near the triple point. Here, we can say that our molecule system is in a transition phase which corresponds to the passage from the gaseous to liquid state. Thus, this transition causes an unbalance into the system. Consequently, our SP_1 values differ from the others.

In addition, our thermodynamic properties especially reduced energy of configuration U^* are in perfect agreement with the experimental data (Sesé, 1993, 1994; Singer and Smith, 1988). However, the reduced total energy E^* agree very well with site–site interaction (Belkacem et al., 2005) and spherical approximation (Tchouar et al., 1998). The results of the dynamic properties: the coefficient of distribution and the viscosity are relative to the stream of particles. These dynamic properties are calculated from the functions of temporal

Table 4 Thermodynamic and transport properties calculated in reduced units. Pressure $P* = P\,\sigma^{-3}/\varepsilon$, Energy of configuration $U* = U/N\varepsilon$, Enthalpy $H* = H/N\varepsilon$, Self-Diffusion Coefficient $D* = D\,(m/\varepsilon)^{1/2}/\sigma$, Viscosity $\eta* = \eta\,\sigma^2/\varepsilon\,(m/\varepsilon)^{1/2}$.

State point	MDBUK	$U*$	$H*$	$P*$	$D*$	$\eta*$
SP$_1$	NVTLNG	−5.4477 ± 0.00720	−6.01700 ± 0.0001	0.2246 ± 0.038	0.168 ± 0.0075	5.756 ± 0.045
	NVTMCRB	−5.305 ± 0.042701	−6.01240 ± 0.0600	0.0804 ± 0.931	0.172 ± 0.0053	5.642 ± 0.035
	NPTMCRB	−5.123 ± 0.042750	−6.01790 ± 0.0130	0.456 ± 0.9319	0.165 ± 0.0042	5.554 ± 0.025
	NVTMCRT	−5.856 ± 0.012500	−5.45900 ± 0.0137	0.371 ± 3.0059	0.248 ± 0.0074	5.975 ± 0.048
	NPTMMCRT	−5.701 ± 0.012570	−5.30425 ± 0.0600	0.371 ± 3.0059	0.264 ± 0.0052	5.824 ± 0.041
SP$_2$	NVTLNG	−6.0466 ± 0.0670	−6.0079 ± 0.072	0.1461 ± 2.755	0.178 ± 0.0079	5.675 ± 0.046
	NVTMCRB	−6.0426 ± 0.0560	−6.0182 ± 0.026	0.0117 ± 0.833	0.174 ± 0.0062	5.544 ± 0.033
	NPTMCRB	−5.0451 ± 0.0780	−6.0082 ± 0.012	0.2633 ± 3.699	0.166 ± 0.0054	5.350 ± 0.023
	NVTMCRT	−5.5060 ± 0.0190	−5.0082 ± 0.012	1.106 ± 3.0460	0.254 ± 0.0054	5.701 ± 0.032
	NPTMCRT	−5.6060 ± 0.0137	−5.0437 ± 0.077	0.1869 ± 3.178	0.2671 ± 0.045	5.701 ± 0.032
SP$_3$	NVTLNG	−6.03170 ± 0.0520	−6.0498 ± 0.060	0.4510 ± 3.069	0.156 ± 0.0056	5.1230 ± 0.044
	NVTMCRB	−6.07020 ± 0.0600	−6.0170 ± 0.058	0.0003 ± 0.694	0.165 ± 0.0523	5.1150 ± 0.032
	NPTMCRB	−5.64027 ± 0.0070	−5.0521 ± 0.082	0.1317 ± 4.812	0.165 ± 0.0054	4.8567 ± 0.025
	NVTMCRT	−5.50670 ± 0.0156	−5.0521 ± 0.083	0.1922 ± 3.235	0.2645 ± 0.004	5.1250 ± 0.042
	NPTMCRT	−5.46350 ± 0.0130	−5.0350 ± 0.016	0.0117 ± 3.608	0.285 ± 0.0032	5.0141 ± 0.032
SP$_4$	NVTLNG	−7.0337 ± 0.0450	−6.0307 ± 0.060	0.1488 ± 2.316	0.235 ± 0.0124	5.0480 ± 0.045
	NVTMCRB	−7.0175 ± 0.0630	−6.0190 ± 0.045	0.0001 ± 0.858	0.235 ± 0.0240	4.7740 ± 0.022
	NPTMCRB	−6.2350 ± 0.0632	−6.0361 ± 0.022	0.123 ± 0.8582	0.2154 ± 0.032	4.7527 ± 0.013
	NVTMCRT	−5.7220 ± 0.0147	−5.0361 ± 0.022	0.217 ± 3.5128	0.345 ± 0.0050	5.0420 ± 0.042
	NPTMCRT	−5.7850 ± 0.0147	−5.0339 ± 0.010	0.217 ± 3.5128	0.3721 ± 0.004	4.9860 ± 0.030
SP$_5$	NVTGNL	−6.0352 ± 0.0070	−6.0309 ± 0.047	0.3869 ± 3.022	0.165 ± 0.045	4.8750 ± 0.044
	NVTMCRB	−6.0098 + 0.0620	−6.0201 ± 0.020	0.0111 ± 0.659	0.356 ± 0.124	4.6520 ± 0.043
	NPTMCRB	−6.0353 ± 0.0077	−6.0301 ± 0.012	0.1936 ± 4.176	0.256 ± 0.154	4.5127 ± 0.024
	NVTMCRT	−5.40278 ± 0.042	−5.0301 ± 0.012	0.3828 ± 2.076	0.385 ± 0.124	4.9560 ± 0.033
	NPTMCRT	−5.3678 ± 0.0106	−5.0267 ± 0.021	0.0010 ± 2.637	0.432 ± 0.012	4.8561 ± 0.030
SP$_6$	NVTLNG	−7.0154 ± 0.0470	−7.0222 ± 0.060	0.0096 ± 0.696	0.254 ± 0.055	4.7560 ± 0.044
	NVTMCRB	−7.0148 ± 0.0630	−7.0231 ± 0.058	0.0052 ± 0.918	0.214 ± 0.056	4.6720 ± 0.031
	NPTMCRB	−6.0346 ± 0.0676	−7.0122 ± 0.018	0.1295 ± 3.927	0.236 ± 0.245	4.5427 ± 0.024
	NVTMCRT	−5.3920 ± 0.0076	−6.0122 ± 0.018	1.7386 ± 2.705	0.4255 ± 0.012	4.8920 ± 0.034
	NPTMCRT	−5.2068 ± 0.0092	−6.0230 ± 0.042	0.0909 ± 2.637	0.4855 ± 0.012	4.7010 ± 0.035
SP$_7$	NVTLNG	−6.0720 ± 0.0380	−7.0675 ± 0.060	0.6201 ± 2.088	0.345 ± 0.2544	4.5230 ± 0.040
	NVTMCRB	−6.0188 ± 0.0640	−7.0260 ± 0.056	0.0757 ± 0.791	0.425 ± 0.2563	3.8750 ± 0.034
	NPTMCRB	−6.0104 ± 0.0715	−7.0280 ± 0.054	0.0868 ± 0.992	0.345 ± 0.2455	3.4577 ± 0.022
	NVTMCRT	−5.0104 ± 0.0668	−6.0280 ± 0.054	1.7101 ± 2.945	0.442 ± 0.0012	4.3260 ± 0.033
	NPTMCRT	−5.1076 ± 0.0797	−6.0179 ± 0.047	0.2025 ± 3.408	0.490 ± 0.0011	4.541 ± 0.0125
SP$_8$	NVTLNG	−6.0346 ± 0.042	−6.0156 ± 0.060	0.3002 ± 2.411	0.4256 ± 0.245	3.5550 ± 0.040
	NVTMCRB	−6.0211 ± 0.055	−7.0270 ± 0.042	0.1020 ± 0.842	0.425 ± 0.231	3.7520 ± 0.031
	NPTMCRB	−6.6249 ± 0.065	−6.0076 ± 0.011	0.0143 ± 3.188	0.321 ± 0.214	2.5487 ± 0.022
	NVTMCRT	−5.3682 ± 0.020	−6.0076 ± 0.011	1.108 ± 3.0410	0.471 ± 0.004	4.2220 ± 0.030
	NPTMCRT	−5.1075 ± 0.073	−6.0168 ± 0.042	0.2175 ± 3.470	0.5055 ± 0.05	3.5241 ± 0.015
SP$_9$	NVTLNG	−6.0104 ± 0.0420	−6.0169 ± 0.063	0.4379 ± 1.944	0.325 ± 0.231	2.9850 ± 0.040
	NVTMCRB	−6.0259 ± 0.0540	−6.0291 ± 0.046	0.087 ± 0.8115	0.231 ± 0.214	2.5260 ± 0.030
	NPTMCRB	−5.3570 ± 0.0555	−6.0311 ± 0.024	0.122 ± 0.8426	0.213 ± 0.123	1.5277 ± 0.027
	NVTMCRT	−5.3116 ± 0.0670	−5.0310 ± 0.024	1.5640 ± 2.642	0.508 ± 0.012	3.1250 ± 0.0272
	NPTMCRT	−5.2150 ± 0.0200	−5.0116 ± 0.067	1.108 ± 3.0410	0.560 ± 0.011	5264 ± 0.031

LNG: liquefied natural gas.
MCRB: multi-component refrigerants for a binary mixture.
MCRT: multi-component refrigerants for a ternary mixture.

correlation. The increase of the temperature induces a net increase of the total energy, the potential energy and the average enthalpy. Therefore, we notice that the values of the pressure are irregular and vary with the temperature and the density of the system. The fluctuations of these properties are weak if compared to classical model (Tchouar et al., 1998). (Table 5).

5. Conclusion

In this work, we have studied many properties for methane–nitrogen and methane–nitrogen–ethane mixtures by molecular dynamics. We have chosen the MD method to predict much better the LNG characteristics. The present calculations con-

Table 5 Comparative study of thermodynamic properties calculated in reduced units for binary and ternary systems.

State point	Method	U^*	E^*	P^*
SP$_1$	MD Buck[a]	-6.901 ± 0.09600	-5.530 ± 0.098	0.053 ± 0.3440
	MD LJ. Jb[b]	-6.460 ± 0.05900	-5.541 ± 0.112	0.024 ± 0.2450
	Exp[c]	–	-5.526	–
	MC LJ. Ja[d]	-6.493 ± 0.06400	-5.577 ± 0.064	0.190 ± 0.3340
	WK (h2)[d]	-6.316 ± 0.06400	-5.434 ± 0.080	0.200 ± 0.2790
	QFH[d]	-6.405 ± 0.06700	-5.405 ± 0.071	0.413 ± 0.3480
	PIMC[d]	-6.408 ± 0.06100	-0.413 ± 0.278	0.396 ± 0.4300
	MD MCRB[e]	-5.123 ± 0.04275	–	0.456 ± 0.9319
	MD MCRT[e]	-5.701 ± 0.01257	–	0.371 ± 3.0059
SP$_4$	MD Buck[a]	-6.825 ± 0.1010	-4.894 ± 0.1025	0.102 ± 0.1470
	MD LJ. Jb[b]	-6.049 ± 0.0240	-4.962 ± 0.0290	0.099 ± 0.1160
	Exp[c]	–	-4.989	–
	MC LJ. Ja[d]	-6.040 ± 0.0670	-4.954 ± 0.067	0.122 ± 0.3480
	WK (h2)[d]	-5.925 ± 0.0710	-4.861 ± 0.086	0.214 ± 0.3120
	QFH[d]	-6.003 ± 0.0670	-4.851 ± 0.069	0.301 ± 0.3380
	PIMC[d]	-6.000 ± 0.0650	-4.853 ± 0.331	0.315 ± 0.4840
	MD MCRB[e]	-6.235 ± 0.0632	–	0.123 ± 0.8582
	MD MCRT[e]	-5.785 ± 0.0147	–	0.217 ± 3.5128
SP$_8$	MD Buck[a]	-6.580 ± 0.2507	-4.424 ± 0.230	0.160 ± 0.0230
	MD LJ. Jb[b]	-5.606 ± 0.0260	-4.348 ± 0.026	0.162 ± 0.0860
	Exp[c]	–	-4.416	–
	MC LJ. Ja[d]	-5.604 ± 0.0710	-4.347 ± 0.071	0.069 ± 0.3450
	WK (h2)[d]	-5.517 ± 0.0730	-4.274 ± 0.086	0.145 ± 0.3110
	QFH[d]	-5.593 ± 0.0680	-4.284 ± 0.071	0.104 ± 0.3320
	PIMC[d]	-5.583 ± 0.0700	-4.281 ± 0.375	0.170 ± 0.4960
	MD MCRB[e]	-5.357 ± 0.0555	–	0.122 ± 0.8426
	MD MCRT[e]	-5.215 ± 0.0201	–	1.108 ± 3.0410

MCRB: multi-component refrigerants for a binary mixture.
MCRT: multi-component refrigerants for a ternary mixture.
[a] Site–site interaction (Belkacem et al., 2005).
[b] Spherical approximation (Tchouar et al., 1998).
[c] Sesé work (Sesé, 1992, 1994).
[d] Experimental work (Sesé, 1992, 1993, 1994).
[e] Our work.

cern the site–site interaction study of 256 particles using the adapted Buckingham potential model. This adapted model allows determining the characteristics for each state point. We have applied this model to study the LNG properties for methane–nitrogen and methane–nitrogen–ethane mixtures by molecular dynamics.

We have calculated the thermodynamic, dynamic and structural properties for both the NVT and NPT ensembles of binary and ternary systems from the SP$_1$ to SP$_9$ points. Then, we have compared the results between binary and ternary systems. We have obtained a good prediction on transport properties for binary and ternary mixtures. The diffusion of methane in the ternary mixture is much better than in the binary mixture. However, the situation for viscosity is reversed.

From the calculated values of self-diffusion coefficient and viscosity, we confirmed that LNG mixture is in liquid state.

We conclude that our simulation model approach very well the experimental data. Our work presents the possibility to determine with a high precision the thermodynamic, dynamics, and structural properties of binary and ternary systems and to propose a good optimisation of the liquefaction process. We hope that this model could be an effectively starting material to study the properties of other complex systems in order to predict the transport phenomenon in the fluids.

References

Allen, M.P., Tildesley, D.J., 1987. Computer Simulation of Liquids. Clarendon Press, Oxford.

Belkacem, F., Krallafa, A., Bormann, D., 2005. J. Soc. Alg. Chem. 15, 35–42.

Berne, B.J., Thirumalai, D.A., 1986. Rev. Phys. Chem. 37, 401–424.

Buckingham, R.A., 1938. Proc R Soc London, A 168A, 264–283.

Catlow, C.R.A., Harker, A.H., Hayns, M.R., 1975. J. Chem. Soc. Faraday Trans. II. 75, 275–285.

Cooper, A.R., 1965. J. Phys. Chem. 6, 55–61.

Dysthe, D.K., Fuchs, A.H., Rousseau, B., 1998. Int. J. Thermophys. 19, 437–448.

Dysthe, D.K., Fuchs, A.H., Rousseau, B., Durandeau, M., 1999. J. Chem. Phys. 110, 4060–4067.

Erpenbeck, J.J., 1988. Phys. Rev. A 38, 6255–6266.

Evens, D.J., Hoover, W.G., 1986. Annu. Rev. Fluid Mech. 18, 243–297.

Evens, D.J., Morriss, G.P., 1984. Comput. Phys. Rep. 1, 297–343.

Habenschuss, A., Johnson, E., Narten, A.H., 1981. J. Chem. Phys. 74, 5234–5241.

Hansen, J.P., McDonald, I.R., 1986. Theory of Simple Liquid, 2nd ed. Academic Press, London.

Kihara, T., 1963. Adv. Chem. Phys. 5, 147.

Kincaid, R.H., Scheraga, H.A., 1982. J. Comp. Chem. 3, 525–547.

Lennard-Jones, J.E., 1924. Proc R Soc London, A 106, 463–477.

Lowden, L.J., Chasndler, D., 1974. J. Chem. Phys. 61, 5228–5241.

Maghri, A., Jalili, A.H., 2004. J. Phys. Soc. Jpn. 73, 1191–1196.

McDonald, I.R., Singer, K., 1972. Mol. Phys. 23, 29.

Mesli, F., Mahboub, R., 2010. Phys. Chem. News. 56.

Mirsky, K., 1978. In: Schenk, Li., OIthoff-Hazekamp, R., Van Koningsveld, H., Bassi, G.C. (Eds.), Computing in Crystallography. Ddelft University, Delft, p. 169.

Morriss, G.P., Daivis, P.J., Evans, D.J., 1991. J. Chem. Phys. 94, 7420–7433.

Murad, S., Evans, D.J., Gubbins, K.E., Street, W.B., Tildesley, D.J., 1979. Mol. Phys. 37, 725.

Nagy, J., Weaver, D.F., Smith, J.R., 1995. J. Mol. Phys. 85, 1179–1192.

Narten, A.H., d, H.A., 1972. In: Franks, F. (Ed.), Waters: A Comprehensive Treatise. Plenum, New York, p. 314.

Nicolas, J.J., Hoheisel, C., Gubbins, K.E., Street, W.B., Tildesley, D.J., 1979. Mol. Phys. 37, 1429–1454.

Padilla, P., Toxvaerd, S., 1992. J. Chem. Phys. 97, 7687–7694.

Powles, J.G., Abascal, J.L.F., 1983. J. Phys. C. 16, 441–444.

Rowlinson, J.S., 1969. Liquids and Liquid Mixtures, 2nd ed. Butterworths, London, p. 51.

Sesé, L.M., 1991. Mol. Phys. 74, 177–189.

Sesé, L.M., 1992. Mol. Phys. 76 (6), 1335–1346.

Sesé, L.M., 1993. Mol. Phys. 78, 1167–1177.

Sesé, L.M., 1994. Mol. Phys. 81, 1297–1312.

Shadman, M., Yeganegi, S., Ziaie, F., 2009. Chem. Phys. Lett. 437, 237–242.

Singer, K., Smith, W., Molec. Phys., 1988, 64, 1215–1231; Morales, J.J., Singer, K., Molec. Phys., 1991, 73, 873–880.

Streett, W.B., Gubbins, K.E., 1977. A. Rev. Phys. Chem. 28, 373–410.

Tchouar, N., Benyamina, D., Lebsir, F., Ould Kaddour, F., Krallafa, A., 1998. Proceeding of the Third Scientific and Technology Conference, SONATRACH. Algiers, Algeria.

Tchouar, N., Benyettou, M., Kadour, F.O., 2003. Int. J Mol Sci. 4, 595–606.

Williams, D.E., 1967. J. Chem. Phys. 47, 4680–4684.

Zhou, Y., Miller, G.H., 1996. J. Phys. Chem. 100, 5516–5524.